International Journal of Solids and Structures 228 (2021) 111128

Contents lists available at ScienceDirect

International Journal of Solids and Structures

journal homepage: www.elsevier.com/locate/ijsolstr

Interaction between the edge dislocation dipole pair and interfacial misfit dislocation network in Ni-based single crystal superalloys

Zhiwei Zhang [a,b], Qiang Fu [c], Jun Wang [a,*], Rong Yang [a], Pan Xiao [a], Fujiu Ke [d], Chunsheng Lu [e]

[a] State Key Laboratory of Nonlinear Mechanics (LNM), Institute of Mechanics, Chinese Academy of Sciences, Beijing 100190, China
[b] School of Engineering Science, University of Chinese Academy of Sciences, Beijing 100049, China
[c] Aero Engine Academy of China, Beijing 101304, China
[d] School of Physics, Beihang University, Beijing 100191, China
[e] School of Civil and Mechanical Engineering, Curtin University, Perth, WA 6845, Australia

ARTICLE INFO

Article history:
Received 26 March 2021
Received in revised form 3 May 2021
Accepted 7 June 2021
Available online 09 June 2021

Keywords:
Ni-based single crystal superalloys
Edge dislocation dipole pair
Interfacial misfit dislocation network
Interacting mechanism
Molecular dynamics

ABSTRACT

Understanding the intrinsic strengthening mechanism is of great significance for microstructural design of Ni-based single crystal superalloys. In this paper, from an atomistic perspective, the interacting mechanism between edge dislocation dipole pair and interfacial misfit dislocation network has been elaborated. It is shown that a network of interfacial misfit dislocations can effectively impede the movement of matrix dislocations, accommodate and pile up the edge dislocation dipole pairs in Ni matrix. Furthermore, we have systematically elucidated the influence of loading rates on the stimulating period of edge dislocation dipole pairs and stiffness of Ni/Ni_3Al substrate. These findings provide a better understanding of the interfacial strengthening mechanism of Ni-based single crystal superalloys.

1. Introduction

Ni-based single crystal superalloys have been widely used in aerospace industries such as for turbine blades and vanes in aircraft engines due to their excellent mechanical performance at high temperatures (Maaß et al., 2012; Yang and Hu, 2014; Jozwik et al., 2015; Khoei et al., 2021). These alloys mainly consist of Ni matrix with face-centered cubic (FCC) structure and dispersion precipitates of Ni_3Al with $L1_2$ structure. Because of non-identical lattice parameters of Ni and Ni_3Al, a stress field results from the lattice mismatch. Obviously, an interface under such a stress field is energetically unstable. Based on the minimum energy principle, atoms on interface rearrange to minimize the stress field between Ni and Ni_3Al phases. Thus, interfacial misfit dislocations (IMDs) are created on interface (Zhu and Yang, 2005; Devincre et al., 2001), which are edge in character and have a burgers vector in the plane of interface. Generally, IMDs that widely exist and form dislocation networks in single crystal superalloys play a crucial role in determining the mechanical properties of Ni-based superalloys. They can absorb and accommodate slip dislocations in Ni matrix, and further impede dislocations in matrix from approaching or cutting themselves (Zhang et al., 2005; Arora et al., 2017; Hussein et al., 2017).

Over the past decades, numerous experiments and computational simulations have been carried out to focus on the structure and evolution of IMD network in Ni-based single crystal superalloys (Lasalmonie and Strudel, 1975; Tian et al., 2000; Zhang et al., 2003, 2004). These studies indicate that yield and creep strengths of Ni-based single crystal superalloys are dependent on the Ni_3Al precipitates and evolution of IMDs at Ni/Ni_3Al interface under various temperatures and loading conditions. Zhang et al. (2004) confirmed that matrix dislocations are prevented from entering and shearing Ni_3Al precipitates due to the strong inhibition effect by IMD networks. Huang et al. (2018) also found that misfit dislocations can effectively hinder rafting of Ni_3Al precipitate and act as barriers to dislocation motion. Therefore, the impediment effect of IMD networks is one of the most important creep strengthening mechanisms of Ni-based single crystal superalloys. Moreover, the structure of a network of Ni/Ni_3Al IMD is dependent on the crystal orientation. On {100}, {110} and {111} planes, patterns of IMD networks are square, rectangle and equilateral triangle, respectively (Xie et al., 2009; Yashiro et al., 2002). Meanwhile, effects of temperature, strain rate, phase interface orientation, and multiaxial stress state on the IMD network evolution have been explored (Wu et al., 2011, 2012a, 2012b; Li et al., 2016). Besides, three-dimensional cubic mosaic models of Ni-based single

* Corresponding author.
E-mail address: wangjun@lnm.imech.ac.cn (J. Wang).

https://doi.org/10.1016/j.ijsolstr.2021.111128
0020-7683/

crystal superalloys were also constructed to observe the network evolution of IMD and to determine their mechanical properties (Tao and Wang, 2006; Chen et al., 2020). Nevertheless, a few works have been done to ascertain the relationship between the microstructural evolution and mechanical properties of Ni-based single crystal superalloys (Yu et al., 2015; Li et al., 2018).

In order to explore the influence of IMD network on mechanical properties, the most important issue is to elaborate its interaction with matrix dislocations. However, matrix dislocations are extremely complicated in the process of plastic deformation, and it is difficult to elucidate the interaction between them. Therefore, various simplified models were used to explore such an interaction. For example, Zhu et al. (2013) explored the interaction mechanism between a single edge dislocation and the Ni/Ni_3Al{1 0 0} IMD network, in which interactive modes, but without {1 1 0} and {1 1 1} IMD networks, were considered. In addition, effects of size and position of voids on the mechanical properties of Ni-based single crystal superalloys have been studied by prefabricating voids at Ni/Ni_3Al interface (Liu et al., 2020; Wang et al., 2019; Shang et al., 2018). However, the interaction between dislocations and IMDs was not interpreted due to a dominating role of voids in plastic deformation. Therefore, to the best of our knowledge, there is still no model to systematically investigate the interaction between complex dislocations and Ni/Ni_3Al IMD networks. The edge dislocation dipole (EDD) as a special structure of complex dislocations, widely exists in plastic deformation of metallic materials. Through simulated nanoindentation, a perfect EDD structure can be constructed in metallic composites (Shuang and Aifantis, 2021). The loading rate in indentation simulation has a significant impact on the mechanical properties of materials (Hána et al., 2020; Lee et al., 2016; Zhang and Zhao, 2013), but its influence on the stimulating period of EDD pairs and stiffness of Ni/Ni_3Al substrate has never been touched.

In this paper, a molecular dynamic method is used to investigate the interaction between EDD pair and ($\bar{1}$10) IMD network in Ni-based single crystal superalloys. The microstructural evolution of EDD pairs and IMD network, indentation force for generation of EDD pairs and interfacial potential energy at Ni/Ni_3Al interface are discussed and analyzed in details. Moreover, effects of loading rates on the stimulating period of EDD pairs and stiffness of Ni/Ni_3Al substrate are also studied.

2. Simulation model and methods

2.1. IMD network of Ni/Ni_3Al heterogeneous interface

As illustrated in Fig. 1a, a heterogeneous interfacial model of Ni/Ni_3Al is constructed for Ni-based single crystal superalloys, which only consists of pure Ni matrix and Ni_3Al precipitate without considering alloying elements such as Ta, Re and Co. As shown in Fig. 1a, three orthogonal coordinates are aligned along with the [11$\bar{2}$], [1 1 1] and [$\bar{1}$10] lattice directions, respectively. To monitor variation of the interfacial potential energy, a thickness of ~ 1.0 nm on both sides of Ni/Ni_3Al interface was surveyed and defined as the "interfacial zone". As is known, lattice misfit corresponds to deformation of an invariant lattice. The mismatch δ is defined as the normalized difference of a lattice parameter between Ni and Ni_3Al phases, that is

$$\delta = 2\frac{\alpha_{\gamma'} - \alpha_{\gamma}}{\alpha_{\gamma'} + \alpha_{\gamma}}, \tag{1}$$

where α_{γ} is 3.52 Å for Ni and $\alpha_{\gamma'}$ is 3.573 Å for Ni_3Al (Kayser and Stassis, 1981; Voter and Chen, 1986). For the Ni/Ni_3Al system, δ is 1.5%. As mismatch exceeds the limit of elasticity, IMD can be formed on interphase interface to reduce distorted energy of the system (Zhu and Wang, 2005). Considering the concept of a coincidence site lattice on misfit interphase interface, such a relationship can be written as

$$n\alpha_{\gamma'} = (n+1)\alpha_{\gamma}, \tag{2}$$

where n is the n-fold of lattice parameter, which is represented as

$$n = \frac{\alpha_{\gamma}}{\alpha_{\gamma'} - \alpha_{\gamma}}. \tag{3}$$

It indicates that within the range of misfit interphase interface, there are at least 66 Ni_3Al lattices and 67 Ni lattices to relax stress induced by the difference of lattice parameters. Therefore, according to misfit parameters, the Ni/Ni_3Al model containing a semicoherent Ni/Ni_3Al interface can be constructed, with a volume of 28.9 × 40.8 × 35.0 nm^3 consisting of ~ 3.7 million atoms.

After energy minimization, to accommodate the misfit strain due to lattice difference between the two phases, a regular quadrilateral IMD network was formed on the ($\bar{1}$10) interface of Ni/Ni_3Al as shown in Fig. 1b. The IMD network consists of three 1/2[0$\bar{1}$1] perfect dislocations and two 1/3[1 0 0] Hirth dislocations at interface, and two 1/6[2$\bar{1}$1] and two 1/6[21$\bar{1}$] Shockley dislocations with four segments of stacking faults in Ni matrix. Inset in Fig. 1b shows the bottom view of ($\bar{1}$10) interface of Ni/Ni_3Al. The distance component along the [1 1 1] direction is 14.0 nm between intersection of two 1/3[1 0 0] Hirth dislocations and a 1/2[0$\bar{1}$1] perfect dislocation. This is matched by the lateral size of a virtual flat indenter in the indentation model to ensure meeting between EDD pairs and IMD network. In the IMD network of Ni/Ni_3Al, only those dislocations with burgers vectors of ⟨1 0 0⟩ Hirth at interface and ⟨1 1 2⟩ Shockley in Ni matrix have dislocation reaction and motion. The 1/2[0$\bar{1}$1] perfect dislocation, however, has less change during relaxation.

2.2. Molecular dynamics simulations

Nanoindentation of Ni/Ni_3Al heterogeneous interfacial models was simulated to investigate generation of EDD pairs and their interaction with IMD network. Fig. 1a shows an initial configuration of Ni/Ni_3Al for indentation simulation. A virtual flat indenter was used with a size of 14.0 × 28.9 nm^2. It only stimulates dislocations along ⟨1 1 2⟩/{1 1 1} slip system due to uniform stress distribution under it. This differs by that with a spherical indenter under which stress distribution is rather nonuniform and various slip systems are activated (Zhang et al., 2021a). To avoid translation in the [110] direction, all samples were restrained by applying a body force distributed uniformly to bottom atoms with a thickness of 1.0 nm. The body force is opposite and equal to that imposed by the indenter. Moreover, the periodic boundary conditions were implemented in [11$\bar{2}$] and [1 1 1] directions, while the [110] direction is kept free. Since the setting of indention simulation continuously generates pure EDD pairs, we can concentrate on their interaction with the IMD network. It also provides the stiffness of Ni/Ni_3Al substrate by fitting its slope at each elastic stage and the stimulating period of EDD pairs between its two neighboring local minimums from the load-depth curve. In particular, these mechanical properties can be analytically expressed.

Atomistic simulations were performed by using the Largescale Atomic/Molecular Massively Parallel Simulator (Plimpton, 1995). The embedded-atom potential function for a Ni − Al system developed by Mishin (2004) was taken to define atomic interactions of Ni and Ni_3Al. In such a function, the total energy,Φ, of a system can be described as

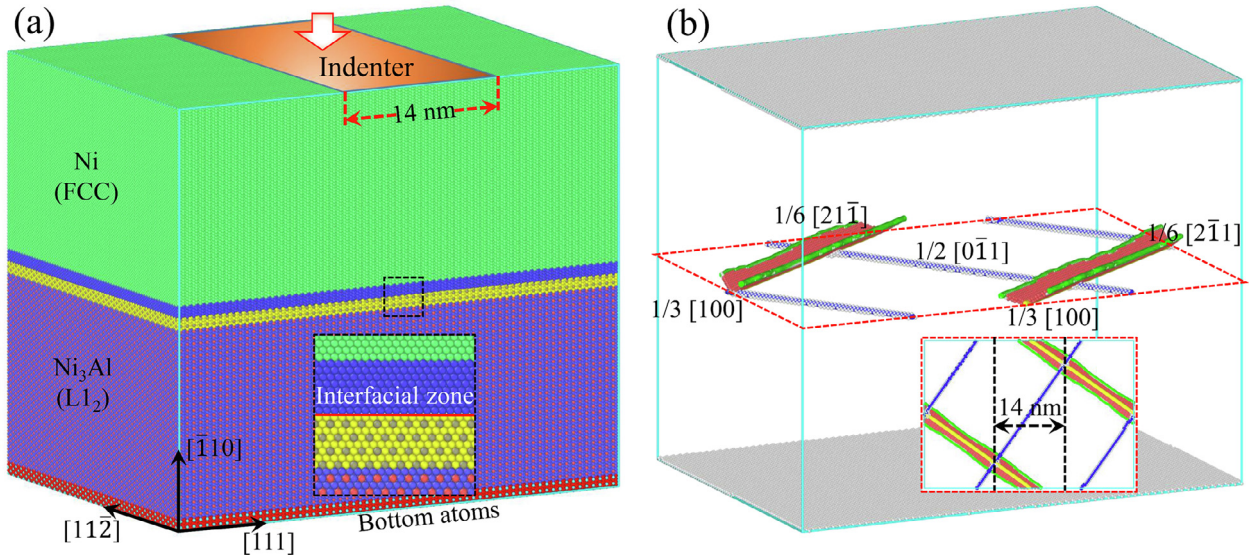

Fig. 1. (a) Sketch of a nanoindentation model for heterogeneous interface of Ni/Ni_3Al to generate EDD pairs, with inset indicating a partially enlarged structure, the plane marked with red line in inset of (a) representing semi-coherent ($\bar{1}10$) interface of Ni/Ni_3Al. (b) The ($\bar{1}10$) IMD network of Ni/Ni_3Al, where atoms are colored by dislocation analysis with white and red representing surface atoms and stacking faults, and green, blue and yellow lines indicating 1/6⟨112⟩ Shockley, 1/2⟨110⟩ perfect and 1/3⟨100⟩ Hirth dislocations, respectively. Inset in (b) shows a bottom view of the IMD network structure. FCC structures were removed for clarity. (For interpretation of the references to colour in this figure legend, the reader is referred to the web version of this article.)

$$\Phi = \sum_{\substack{i,j \\ i \neq j}} \varphi_{EAM}(r_{ij}) + \sum_i F(\bar{\rho}_i), \tag{4}$$

where $\varphi_{EAM}(r_{ij})$ is a pair interaction energy represented as a function of the distance r_{ij} between atoms i and j, and F is the embedding energy of atom i, and $\bar{\rho}_i$ is the function of electron density, which is given by

$$\bar{\rho}_i = \sum_{i \neq j} f_j(r_{ij}), \tag{5}$$

where $f_j(r_{ij})$ is the electron density of atom j.

Simulations were carried out by integrating Newton's equations of motion for all atoms with a time step of 2 fs. At the start of simulations, initial configurations were energetically minimized by relaxing all samples for 50 ps. Temperature was controlled at 1 K during simulations to avoid thermal effects. Indentation loading rates were 1, 5 and 10 m s^{-1} and the maximum indentation depth was 2 nm. Deformation and defects of Ni/Ni_3Al were recognized via the common neighbor and dislocation analysis and then, they were visualized with software OVITO (Stukowski, 2010).

3. Results

3.1. Nucleation of EDD pairs during indentation

Outwardly, the indentation force-indentation depth curve of Ni/Ni_3Al substrate with a loading rate of 5 m s^{-1} can be divided into four stages via monitoring the indentation force, interfacial potential energy and dislocation activities (see Fig. 2). To maintain the integrity of Ni/Ni_3Al IMD network, the virtual flat indenter is embedded in Ni matrix during the initial indentation stage with a depth of 2.5 Å, i.e., $\frac{\sqrt{2}\alpha_{Ni}}{2}$. This leads to a nonzero, but false, initial indentation force in stage I. In stage II, the indentation force-depth curve of Ni/Ni_3Al first undergoes an upward trend until indentation depth reaching to 0.27 nm (point A in Fig. 2) at which an EDD pair is nucleated (see Fig. 4a). Each EDD is composed of two 1/6⟨112⟩ Shockley dislocations and a slice of stacking fault

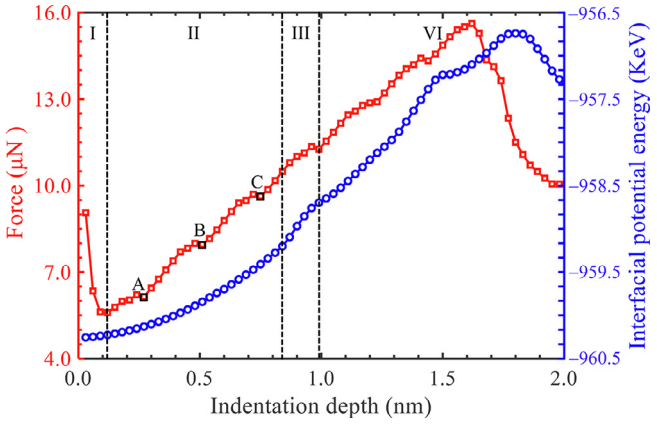

Fig. 2. Typical indentation force- and interfacial potential energy-indentation depth curves of Ni/Ni_3Al substrate. Points A – C mark three successively generating events of EDD pairs.

between them. Formation of an EDD pair follows two steps. First, under indentation, two 1/6⟨112⟩ Shockley dislocations are generated along the {111} slip plane with two stacking faults behind them adhering to the lower surface of Ni matrix. Then, with the increase of indentation depth, the other two 1/6⟨112⟩ Shockley dislocations nucleate to terminate the two stacking faults and the first EDD pair is formed (Its structure is shown in Fig. 3). The spacing between two components of an EDD pair is 14 nm, resulting from the lateral dimension of the virtual flat indenter.

As indentation depth increases to 0.51 nm, the second EDD pair separates from surface of Ni matrix and indentation force drops to its local minimum (point B in Fig. 2). Fig. 4b shows the structure of two EDD pairs and IMD network. At that moment, the first EDD pair moves toward IMD network with its structure keeping unchanged. After that, with the increase of indentation depth, the indentation force grows again to its local maximum where the third EDD pair begins to nucleate. Separation of the third EDD pairs from surface witnesses a drop of indentation force to its local minimum once more at an indentation depth of 0.75 nm

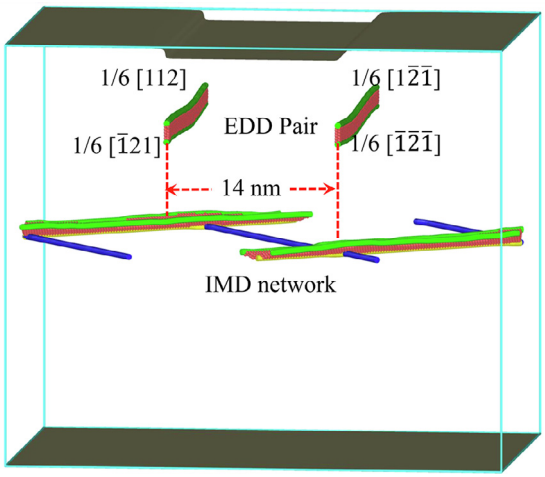

Fig. 3. Microstructure of the first EDD pair and ($\bar{1}$10) IMD network, where atoms are colored by common neighbor and dislocation analysis. FCC and surface atoms are omitted for clarity.

(marked as C in Fig. 2). Then, three EDD pairs move downwardly in coordination (see Fig. 4c). As the first EDD pair is close to IMD network, the latter undergoes partial structural change due to a repulsive force between them. The original 1/6⟨112⟩ Shockley dislocations belonging to IMD network expand along ⟨112⟩/(111) slip system in the Ni matrix, accompanied by deformation of partial stacking faults. Meanwhile, part of each 1/3[100] Hirth dislocation of the IMD network decomposes to 1/6⟨112⟩ Shockley dislocations at interface and gradually expands in Ni_3Al precipitate (see the amplified region in Fig. 4c). The reaction can be expressed as 1/3[100] → 1/6[112] + 1/6[112]. The interface potential energy shows a monotonic upward trend in entire stage II as EDD pairs gradually approach IMD network.

3.2. Interaction between EDD pair and IMD network

To understand the interaction between EDD pair and IMD network, dislocation reaction and motion as well as interfacial deformation were analyzed. As the indentation depth reaches 0.75 nm (see Fig. 4c), the first EDD pair approaches IMD network, so that the interfacial network plane is subjected to a repulsive force to undergo a slight structural change. In stage III of Fig. 2, at an indentation depth of 0.90 nm, the first EDD pair contacts and reacts with IMD network. At the same time, the second and third EDD pairs also move downward (see Fig. 5a). Because the first EDD pair adheres to the IMD network plane, resulting in dislocations belonging to the latter to decompose and redistribute on both sides of interface. This process embodies an obvious turning point on the interfacial potential energy-depth curve (see Fig. 2). The IMD network reacts with the first EDD pair to produce the dislocation pinning lock, which blocks its continuous movement. As indentation depth continues to increase, the first EDD pair is completely embedded in IMD network, generating more dislocation pinning points. Meanwhile, more EDD pairs generated from indentation surface continuously move downward and accumulate on IMD network to pile up above Ni/Ni_3Al interface. Below Ni/Ni_3Al interface, several 1/6⟨112⟩ Shockley dislocations decomposed from IMD network gradually begin to expand in Ni_3Al precipitate (see Fig. 5b and c). With indentation depth further increasing, the first EDD pair cuts in IMD network, and basically maintains its original structure. This causes a large number of 1/6⟨112⟩ Shockley dislocations attaching to the first EDD pair, contacting and interacting with each other to form several dislocation pinnings to impede motion of EDD pairs (see Fig. 5d and e). However, there are still some 1/6⟨112⟩ Shockley dislocations from decomposition of IMD network that spread inside Ni_3Al precipitate (see Fig. 5f).

As indentation depth continues to increase, more EDD pairs generated from indentation surface continuously move downward, and two EDD pairs pass through IMD network (see Fig. 6a), corresponding to indentation force reaching to its peak value (see Fig. 2). Subsequently, the indentation force-indentation depth curve shows a downward trend with indentation depth further increases. The interface potential energy-indentation depth curve also reaches its peak value as indentation depth arrives to1.80 nm. After that, newly generated EDD pairs have piled up and merged below indentation surface, and finally collapsed by themselves (see Fig. 6b). Here, it is worth noting that three 1/2[0$\bar{1}$1] perfect dislocations in IMD network do not move any more. They maintain the dislocation pinning state during whole indentation processes. The detailed dislocations dynamic evolution process with a loading rate of 5 m s^{-1} can be found in Video S1.

3.3. Influence of loading rates

Indentation force-indentation depth curves are shown in Fig. 7a to illustrate the effect of loading rates on generation of EDD pairs and their interaction with IMD network. As shown in Fig. 7a, the stimulating period of EDD pairs decreases from 157.5 to 26 ps as the loading rate increases from 1 to 10 m s^{-1} (see Table 1). Meanwhile, the number of EDD pairs generated decreases with the increase of loading rate at the same indentation depth. However, the average stiffness of Ni/Ni_3Al substrate is positively related to

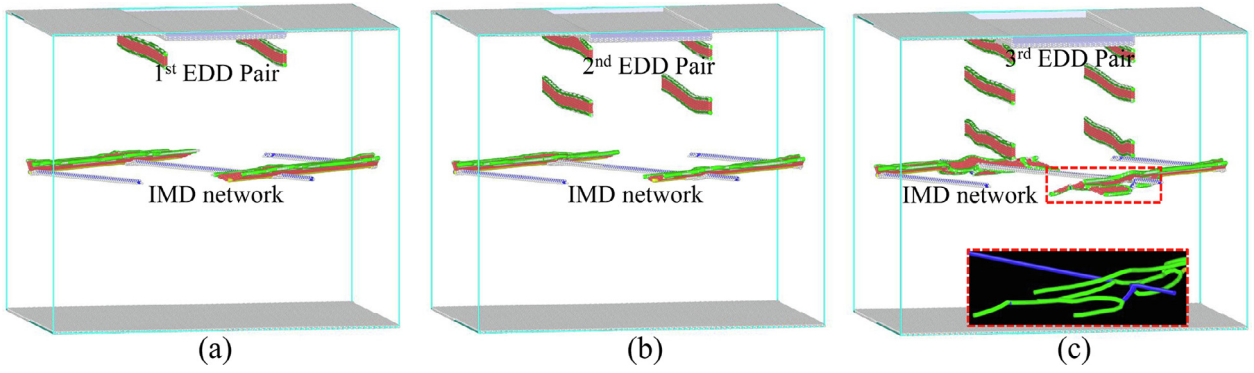

Fig. 4. Atomic configurations at various indentation depths of (a) 0.27, (b) 0.51 and (c) 0.75 nm, where atoms are colored by common neighbor and dislocation analysis, with green, blue and yellow lines indicating 1/6⟨112⟩ Shockley, 1/2⟨110⟩ perfect, and 1/3⟨100⟩ Hirth dislocations, respectively. Inset in (c) indicates a partially enlarged structure colored by dislocation analysis. (For interpretation of the references to colour in this figure legend, the reader is referred to the web version of this article.)

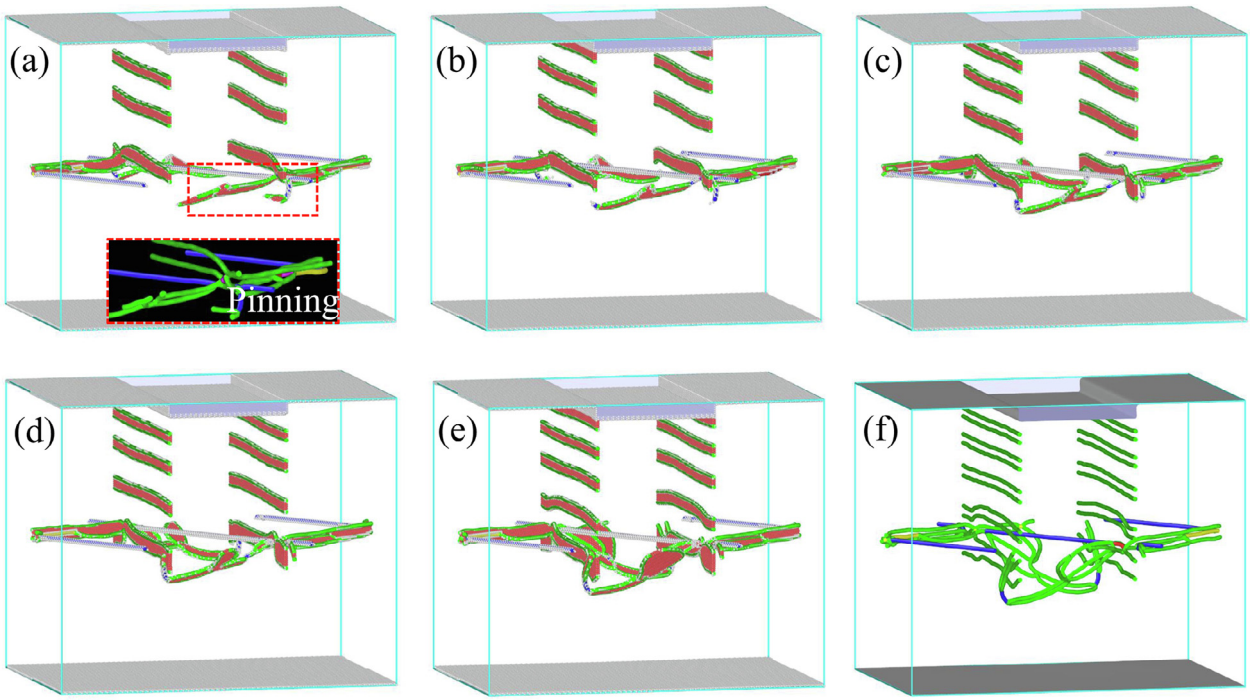

Fig. 5. Evolution of dislocations and structure for interaction between an EDD pair and IMD network with various indentation depths of (a) 0.90, (b) 0.96, (c) 1.02, (d) 1.08, (e) 1.20 and (f) 1.29 nm. Inset in (a) indicates a partially enlarged structure colored by dislocation analysis.

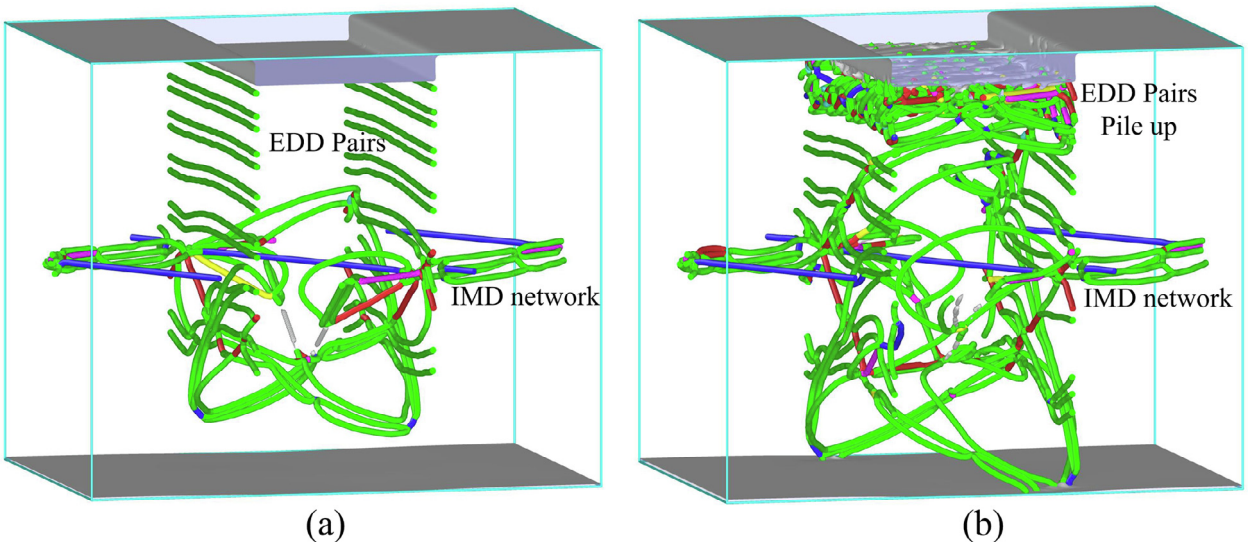

Fig. 6. Dislocation patterns of EDD pairs and Ni/Ni_3Al IMD network at various indentation depths of (a) 1.62 and (b) 1.80 nm, where atoms are colored by dislocation analysis, with green, blue, purple, yellow and red lines representing 1/6⟨112⟩ Shockley, 1/2⟨110⟩ perfect, 1/6⟨110⟩ stair-rod, 1/3⟨100⟩ Hirth, and other kinds of dislocations, respectively. (For interpretation of the references to colour in this figure legend, the reader is referred to the web version of this article.)

loading rate. Here, an average stiffness is obtained from an indentation force-depth curve by measuring slopes of every episode in which an EDD pair is generated. Corresponding values of average stiffness of Ni/Ni_3Al substrate are 7169.0, 8498.6 and 10703.3 N m^{-1} for loading rates of 1, 5 and 10 m s^{-1}, respectively. The interfacial potential energy-indentation depth curves reflect the interaction between EDD pairs and IMD network (See Fig. 7b). It is seen that, with the loading rate of 1 m s^{-1}, the amount of EDD pairs generated is more than that under the other two loading rates. Each turning point of interfacial potential energy-indentation depth curves represents the interaction between an EDD pair and the IMD network, which results in the interface potential energy with an increase trend in local regions. However, as the loading rate reaches 10 m s^{-1}, only four integral EDD pairs are generated within the indentation depth of 2 nm. Before further generating events, three of them have piled up and collapsed by themselves below the surface of Ni matrix. Therefore, the corresponding interfacial potential energy-indentation depth curve just has one turning point in the rising phase, representing only once interaction between the first EDD pair and IMD network.

Fig. 8 shows the microstructural evolution of IMD network and EDD pairs during interacting processes with various loading rates.

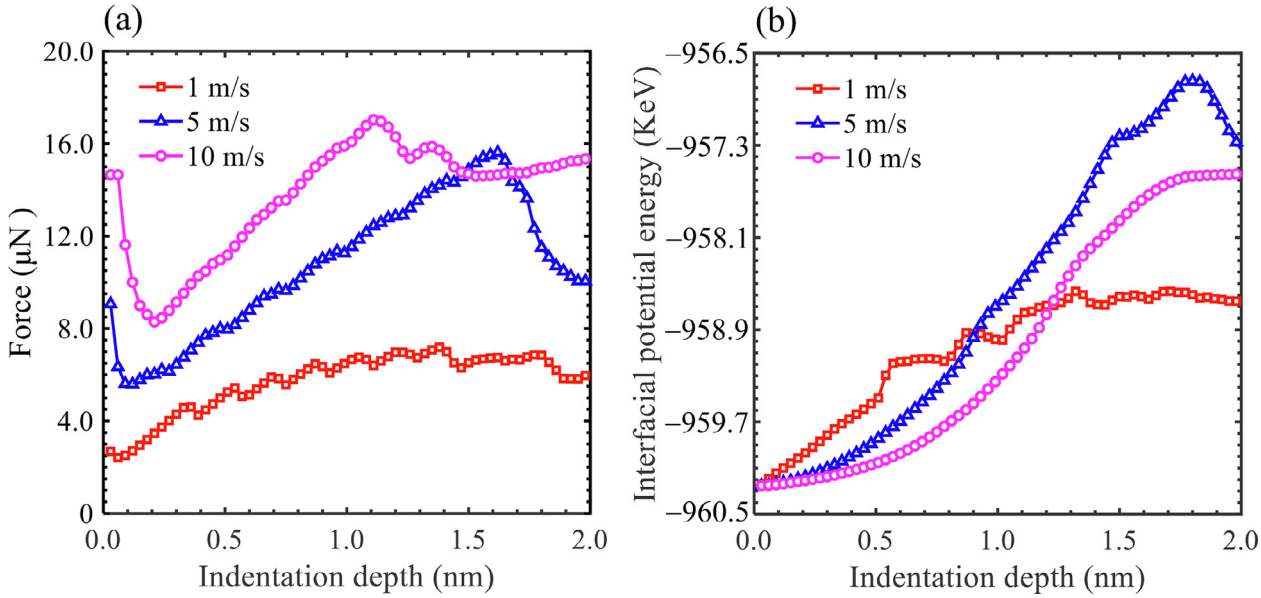

Fig. 7. (a) Indentation force-indentation depth curves and (b) interfacial potential energy-indentation depth of Ni/Ni_3Al substrate with various loading rates.

Table 1
Indentation stiffness of Ni/Ni_3Al substrate and the stimulating period of EDD pairs under different loading rates, where values in brackets are the theoretical predictions by Eq. (7).

Loading rate v_l(m s^{-1})	Stiffness of the Ni/Ni_3Al substrate k (N m^{-1})	Stimulated period of EDD pairs τ(ps)
1	7169.0	157.5 [144.7]
5	8498.6	46.8 [26.6]
10	10703.3	26.0 [11.8]

It is seen that at a loading rate of 1 m s^{-1}, their interaction can easily cause dislocation decomposition of the former, and expansion of several 1/6⟨1 1 2⟩ Shockley dislocations in Ni_3Al precipitate (see Fig. 8a). As the loading rate reaches 5 m s^{-1}, dislocations and stacking faults are mainly concentrated in the region around interface, slightly extending into Ni_3Al precipitate (see Fig. 8b). However, as loading rate raises to 10 m s^{-1}, only the first EDD pair contacts with IMD network, with subsequent generated three EDD pairs piling up, merging and collapsing by themselves within Ni matrix (see Fig. 8c). The whole dynamic evolution process of interaction between EDD pairs and IMD network with loading rates of 1 and 10 m s^{-1} can be found in Videos S2 and S3, respectively.

4. Discussion

4.1. Interaction between EDD pair and IMD network

As mentioned above, successively emitted EDD pairs are considered to model the interaction between them and IMD network of Ni-based single crystal superalloys with various loading rates. It is shown that the IMD network can effectively impede, accommodate and pile up EDD pairs in Ni matrix, which has a positive effect on the mechanical properties of superalloys. The results are consistent with previous works depicting motion and expansion of matrix dislocations during a high temperature creep process of Ni-based single crystal superalloys (Chen et al., 2020; Yu et al., 2015; Li et al., 2018; Zhu et al., 2013; Xia et al., 2020). The interaction between EDD pairs and IMD network leads to generation of dislocation pinning locks in interfacial network. It also results in decomposition of dislocations belonging to IMD network and this induces excitation and propagation of new 1/6⟨1 1 2⟩ Shockley dislocations in Ni_3Al precipitate. Moreover, EDD pairs piling up, merging and collapsing by themselves above Ni/Ni_3Al interface directly reflect that IMD network has a good ability to block motion of dislocations and absorb matrix dislocations. This ability is helpful to improve the mechanical properties of Ni-based single crystal superalloys, and also echoes the finding that heterogeneous inter-

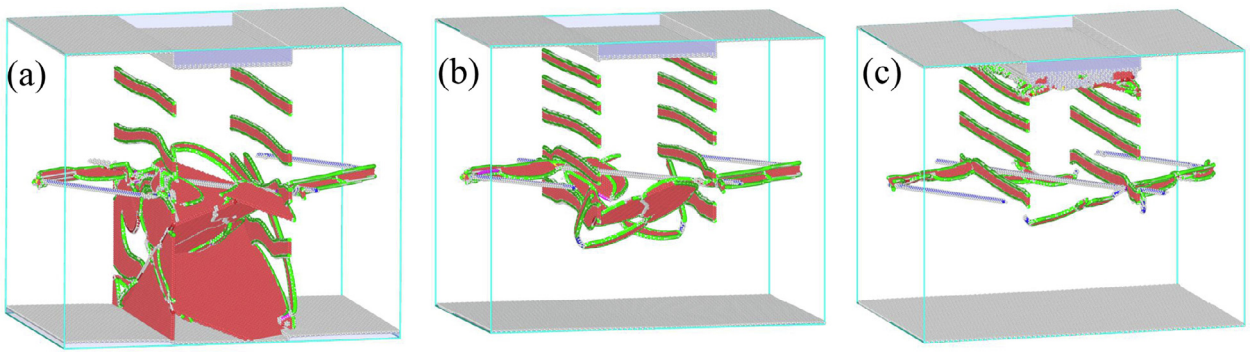

Fig. 8. Microstructural evolution of Ni/Ni_3Al IMD network and EDD pairs during the interacting process at an indentation depth of 1.35 nm with loading rates of (a) 1, (b) 5 and (c) 10 m s^{-1}.

face can effectively improve strength and ductility of nanostructured materials (Zhang et al., 2021a, 2021b; Sathiyamoorthi and Kim, 2020).

4.2. Theoretical model of loading rates

At a given temperature, a dislocation has a certain speed. Since the virtual flat indenter moves uniformly and only $\langle 1\,1\,2\rangle/\{1\,1\,1\}$ slip system is activated, EDD pairs are, therefore, periodically generated with the same spacing. It is also shown that the generating period of EDD pairs is significantly depends on the loading rates. At a lower loading rate, the stimulating period of EDD pair is relatively longer, while the stiffness of Ni/Ni_3Al substrate is relatively smaller. At a higher loading rate, they are just opposite. To explain loading rate effects on the stimulating period of EDD pairs and stiffness of Ni/Ni_3Al substrate, a theoretical model of loading rate effects was constructed by energy analysis. The formation energy of an EDD pair can be divided into two parts. One is the formation energy of four $1/6\langle 1\,1\,2\rangle$ Shockley dislocations, $N\Delta\xi$, where N = 1850 is the number of atoms contained in four Shockley dislocation lines, which can be directly counted from a simulating configuration. $\Delta\xi$ is the activation energy of $1/6\langle 1\,1\,2\rangle$ Shockley dislocation, and its value ranges from 0.2 to 0.3 eV (Parthasarathy and Dimiduk, 1996). Here, we adopt $\Delta\xi$ = 0.25 eV. The other is the formation energy of two stacking faults, $2bL_x\mu$, between two $1/6\langle 1\,1\,2\rangle$ Shockley dislocation lines, where b is the magnitude of burgers vector of $1/6\langle 1\,1\,2\rangle$ Shockley in Ni matrix, μ= 125 mJ m^{-2} represents stacking fault energy of Ni (Angelo et al., 1995), and L_x = 28.9 nm indicates the size of Ni/Ni_3Al substrate in the $[11\bar{2}]$-direction. Let us assume that a stimulating period of EDD pairs is τ and the indenter loading rate is v_l. Thus, in the stimulating period, the indenter moves a distance of $v_l\tau$. Given that the stiffness of substrate is k, external work has to satisfy the formation energy of an EDD pair, that is

$$\frac{1}{2}k(v_l\tau)^2 = N\Delta\xi + 2bL_x\mu, \tag{6}$$

which indicates that the stiffness of Ni/Ni_3Al substrate and stimulating period of EDD pairs are coupled together. Rearranging Eq. (6), the stimulating period of EDD pairs can be written as

$$\tau = \frac{1}{v_l}\sqrt{\frac{2N\Delta\xi + 4bL_x\mu}{k}}. \tag{7}$$

Then, the stimulating periods of EDD pairs for loading rates of 1, 5 and 10 m s^{-1} are derived as 144.7, 26.6, and 11.8 ps, respectively (see Table 1). It is seen that, at a loading rate of 1 m s^{-1}, the theoretical prediction value is consistent with simulation. However, theoretical values are lower than that of simulating results at loading rates of 5 and 10 m s^{-1}. This is due to the inaccuracy of stiffness measured at higher loading rates because a few EDD pairs can be generated without collapse by themselves.

5. Conclusions

In summary, by using molecular dynamics nanoindentation simulations, perfect EDD pairs have firstly been constructed in Ni matrix, and then, interaction mechanisms have been investigated between EDD pairs and IMD network in Ni-based single crystal superalloys. It is shown that, the IMD network has an ability to impede, accommodate and pile up EDD pairs in Ni matrix. The higher the loading rate is, the more obvious this ability is. The main conclusions can be summarized as follows:

(1) The interaction between EDD pairs and IMD network leads to generation of dislocation pinning locks in an interfacial network. It also results in decomposition of dislocations belonging to the IMD network, which induces excitation and propagation of new $1/6\langle 1\,1\,2\rangle$ Shockley dislocations in Ni_3Al precipitate.
(2) Moreover, EDD pairs piling up, merging and collapsing by themselves above Ni/Ni_3Al interface directly reflect that the IMD network has a good ability to block motion of dislocations and absorb matrix dislocations.
(3) In contrast to the stiffness of Ni/Ni_3Al substrate, the stimulating period of EDD pairs is negatively interrelated with loading rate. The stimulating period of EDD pairs decreases from 157.5 to 26 ps as the loading rate increases from 1 to 10 m s^{-1}, its theoretical prediction value is consistent with the simulation result at a loading rate of 1 m s^{-1}. However, the theoretical values are lower than that of simulating results at loading rates of 5 and 10 m s^{-1} due to the inaccuracy of stiffness measured at higher loading rates.

It is expected that these findings could contribute to a deep understanding of intrinsic strengthening mechanisms and the microstructural design of Ni-based single crystal superalloys and other nanostructured materials with heterogeneous interfaces.

6. Data availability

The data that support the findings within this paper are available from the corresponding authors upon reasonable request.

CRediT authorship contribution statement

Zhiwei Zhang: Conceptualization, Investigation, Methodology, Data curation, Writing - original draft. **Qiang Fu:** Formal analysis. **Jun Wang:** Conceptualization, Supervision, Funding acquisition. **Rong Yang:** Funding acquisition. **Pan Xiao:** Methodology, Funding acquisition. **Fujiu Ke:** Methodology. **Chunsheng Lu:** Conceptualization.

Declaration of Competing Interest

The authors declare that they have no known competing financial interests or personal relationships that could have appeared to influence the work reported in this paper.

Acknowledgements

This work has been supported by the National Natural Science Foundation of China (Grant Nos. 11772332 and 11790292), the Strategic Priority Research Program of the Chinese Academy of Sciences (Project No. XDB22040501), and the Opening Fund of State Key Laboratory of Nonlinear Mechanics. The simulations were performed on resources provided by the ScGrid of Supercomputing Center, Computer Network Information Center of the Chinese Academy of Sciences, the LNMGrid of the State Key Laboratory of Nonlinear Mechanics and the Pawsey Supercomputing Center with funding from the Australian Government and the Government of Western Australia.

Appendix A. Supplementary data

Supplementary data to this article can be found online at https://doi.org/10.1016/j.ijsolstr.2021.111128.

References

Angelo, J.E., Moody, N.R., Baskes, M.I., 1995. Trapping of hydrogen to lattice defects in nickel. Model. Simul. Mater. Sci. Eng. 3 (3), 289–307.

Arora, K., Kishida, K., Tanaka, K., Inui, H., 2017. Effects of lattice misfit on plastic deformation behavior of single-crystalline micropillars of Ni-based superalloys. Acta Mater. 138, 119–130.

Chen, B., Wu, W.-P., Chen, M.-X., Guo, Y.-F., 2020. Molecular dynamics study of fatigue mechanical properties and microstructural evolution of Ni-based single crystal superalloys under cyclic loading. Comput. Mater. Sci. 185, 109954. https://doi.org/10.1016/j.commatsci.2020.109954.

Devincre, B., Kubin, L.P., Lemarchand, C., Madec, R., 2001. Mesoscopic simulations of plastic deformation. Mater. Sci. Eng. A 309-310, 211–219.

Hána, T., Vokáč, M., Eliášová, M., V. Machalická, K., 2020. Experimental investigation of temperature and loading rate effects on the initial shear stiffness of polymeric interlayers. Eng. Struct. 223, 110728. https://doi.org/10.1016/j.engstruct.2020.110728.

Huang, S., Huang, M.S., Li, Z.H., 2018. Effect of interfacial dislocation network on the evolution of matrix dislocations in nickel-based superalloy. Int. J. Plast. 110, 1–18.

Hussein, A.M., Rao, S.I., Uchic, M.D., Parthasarathy, T.A., El-Awady, J.A., 2017. The strength and dislocation microstructure evolution in superalloy microcrystals. J. Mech. Phys. Solids 99, 146–162.

Jozwik, P., Polkowski, W., Bojar, Z., 2015. Applications of Ni_3Al based intermetallic alloys–current stage and potential perceptivities. Materials 8 (5), 2537–2568.

Kayser, F.X., Stassis, C., 1981. The elastic constants of Ni_3Al at 0 and 23.5 °C. Phys. Status Solidi A 64 (1), 335–342.

Khoei, A.R., Eshlaghi, G.T., Shahoveisi, S., 2021. Atomistic simulation of creep deformation mechanisms in nickel-based single crystal superalloys. Mater. Sci. Eng. A 809, 140977. https://doi.org/10.1016/j.msea.2021.140977.

Lasalmonie, A., Strudel, J.L., 1975. Interfacial dislocation networks around γ′ precipitates in nickel-base alloys. Philos. Mag. 32 (5), 937–949.

Lee, J., Kim, Y.S., Chae, D., Cho, W., 2016. Loading rate effects on strength and stiffness of frozen sands, KSCE. J. Civ. Eng. 20 (1), 208–215.

Li, N.-L., Wu, W.-P., Nie, K., 2018. Molecular dynamics study on the evolution of interfacial dislocation network and mechanical properties of Ni-based single crystal superalloys. Phys. Lett. A 382 (20), 1361–1367.

Li, Y.-L., Wu, W.-P., Ruan, Z.-G., 2016. Molecular dynamics simulation of the evolution of interfacial dislocation network and stress distribution of a Ni-based single-crystal superalloy, Acta Metall. Sin.-Engl. 29 (7), 689–696.

Liu, H., Wang, X.M., Liang, H., Zhao, Z.N., Li, L., Yue, Z.F., Deng, C.H., 2020. The effect of void defect on the evolution mechanisms of dislocations and mechanical properties in nickel-based superalloys by molecular dynamics simulation of real γ/γ′ structures. Int. J. Solids Struct. 191-192, 464–472.

Maaß, R., Meza, L., Gan, B., Tin, S., Greer, J.R., 2012. Ultrahigh Strength of Dislocation−Free Ni_3Al Nanocubes. Small 8 (12), 1869–1875.

Mishin, Y., 2004. Atomistic modeling of the γ and γ′-phases of the Ni−Al system. Acta Mater. 52 (6), 1451–1467.

Parthasarathy, T.A., Dimiduk, D.M., 1996. Atomistic simulations of the structure and stability of "PPV" locks in an $L1_2$ compound. Acta Mater. 44 (6), 2237–2247.

Plimpton, S., 1995. Fast parallel algorithms for short-range molecular dynamics. J. Comput. Phys. 117 (1), 1–19.

Sathiyamoorthi, P., Kim, H.S., 2020. High-entropy alloys with heterogeneous microstructure: processing and mechanical properties. Prog. Mater. Sci. 100709.

Shang, J., Yang, F., Li, C., Wei, N., Tan, X., 2018. Size effect on the plastic deformation of pre-void Ni/Ni_3Al interface under uniaxial tension: A molecular dynamics simulation. Comput. Mater. Sci. 148, 200–206.

Shuang, F., Aifantis, K.E., 2021. Dislocation-graphene interactions in Cu/graphene composites and the effect of boundary conditions: a molecular dynamics study. Carbon 172, 50–70.

Stukowski, A., 2010. Visualization and analysis of atomistic simulation data with OVITO-the Open Visualization Tool. Model. Simul. Mater. Sci. Eng. 18 (1), 015012. https://doi.org/10.1088/0965-0393/18/1/015012.

Tao, Z., Wang, C.Y., 2006. Molecular dynamics study of mosaic structure in the Ni-based single-crystal superalloy. Chin. Phys. 15 (9), 2087–2091.

Tian, S.G., Zhou, H.H., Zhang, J.H., Yang, H.C., Xu, Y.B., Hu, Z.Q., 2000. Formation and role of dislocation networks during high temperature creep of a single crystal nickel-base superalloy. Mater. Sci. Eng. A 279 (1-2), 160–165.

Voter, A.F., Chen, S.P., 1986. Accurate interatomic potentials for Ni, Al and Ni_3Al. MRS Proc. 82, 175.

Wang, J.P., Liang, J.W., Wen, Z.X., Yue, Z.F., 2019. Atomic simulation of void location effect on the void growth in nickel-based single crystal. Comput. Mater. Sci. 160, 245–255.

Wu, W.P., Guo, Y.F., Wang, Y.S., 2012a. Evolution of misfit dislocation network and tensile properties in Ni-based superalloys: a molecular dynamics simulation. Sci. China Phys. Mech. Astron. 55 (3), 419–427.

Wu, W.P., Guo, Y.F., Wang, Y.S., 2012b. Influence of stress state on the evolution of misfit dislocation networks in a Ni-based single crystal superalloy. Philos. Mag. 92 (12), 1456–1468.

Wu, W.P., Guo, Y.F., Wang, Y.S., Mueller, R., Gross, D., 2011. Molecular dynamics simulation of the structural evolution of misfit dislocation networks at γ/γ′ phase interfaces in Ni-based superalloys. Philos. Mag. 91 (3), 357–372.

Xia, W.S., Zhao, X.B., Yue, L., Zhang, Z., 2020. Microstructural evolution and creep mechanisms in Ni-based single crystal superalloys: A review. J. Alloys Compd. 819, 152954. https://doi.org/10.1016/j.jallcom.2019.152954.

Xie, H.X., Wang, C.Y., Yu, T., 2009. Motion of misfit dislocation in a Ni/Ni_3Al interface: a molecular dynamics simulations study. Model. Simul. Mater. Sci. Eng. 17, 055007.

Yang, X., Hu, W., 2014. The alloying element dependence of the local lattice deformation and the elastic properties of Ni_3Al: A molecular dynamics simulation. J. Appl. Phys. 115 (15), 153507. https://doi.org/10.1063/1.4870235.

Yashiro, K., Naito, M., Tomita, Y., 2002. Molecular dynamics simulation of dislocation nucleation and motion at γ/γ′ interface in Ni-based superalloy. Int. J. Mech. Sci. 44 (9), 1845–1860.

Yu, J.G., Zhang, Q.X., Yue, Z.F., Liu, R., Tang, M.K., Li, X.W., 2015. Microstructure evolution and mechanical behavior of the Ni/Ni_3Al interface under thermal-mechanical coupling. Mater. Express 5, 343–350.

Zhang, J.X., Murakumo, T., Koizumi, Y., Kobayashi, T., Harada, H., 2004. Strengthening by γ/γ′ interfacial dislocation networks in TMS-162—toward a fifth-generation single-crystal superalloy. Metall. Mater. Trans. A 35 (6), 1911–1914.

Zhang, J.X., Murakumo, T., Harada, H., Koizumi, Y., 2003. Dependence of creep strength on the interfacial dislocations in a fourth generation SC superalloy TMS-138. Scr. Mater. 48 (3), 287–293.

Zhang, J.X., Wang, J.C., Harada, H., Koizumi, Y., 2005. The effect of lattice misfit on the dislocation motion in superalloys during high-temperature low-stress creep. Acta Mater. 53 (17), 4623–4633.

Zhang, Q.B., Zhao, J., 2013. Effect of loading rate on fracture toughness and failure micromechanisms in marble. Eng. Fract. Mech. 102, 288–309.

Zhang, Z., Fu, Q., Wang, J., Xiao, P., Ke, F., Lu, C., 2021a. Hardening Ni_3Al via complex stacking faults and twinning boundary. Comput. Mater. Sci. 188, 110201.

Zhang, Z.W., Fu, Q., Wang, J., Yang, R., Xiao, P., Ke, F.J., Lu, C.S., 2021. Interactions between butterfly-like prismatic dislocation loop pairs and planar defects in Ni_3Al, Phys. Chem. Chem. Phys. 23, 10377–10383.

Zhu, T., Wang, C.Y., 2005. Misfit dislocation networks in the γ/γ′ phase interface of a Ni-based single-crystal superalloy: Molecular dynamics simulations. Phys. Rev. B 72, 014111.

Zhu, Y., Li, Z., Huang, M., 2013. Atomistic modeling of the interaction between matrix dislocation and interfacial misfit dislocation networks in Ni-based single crystal superalloy. Comput. Mater. Sci. 70, 178–186.